JOURNAL OF MATERIALS SCIENCE 41 (2006) 53–63

# Flexoelectric effects: Charge separation in insulating solids subjected to elastic strain gradients

L. ERIC CROSS
*Evan Pugh Professor Emeritus of Electrical Engineering, The Materials Research Institute, Pennsylvania State University, University Park, PA 16802, USA*

After a brief historical introduction this article will present a summary of experimental work carried through at Penn State to explore the flexoelectric coefficients $\mu_{ijkl}$ in ferroelectric, incipient ferroelectric and relaxor ferroelectric perovskites. The initial objective was to understand the magnitude of flexoelectricity in these systems to see whether it would be possible to develop a piezoelectric composite containing no piezoelectric element, which nonetheless could have practically useful properties. Recent discussions of the thermodynamic converse effect, ie. the generation of elastic strain by an electric field gradient, now suggest that such composites might be designed to have unique properties such as a direct but no converse effect, or vice-versa, and materials with this character could have important practical application. Present data already suggest that the direct effect may make an important contribution to the properties of epitaxial thin films where mismatch can give rise to very steep elastic strain gradients. Clearly, more work is needed to fully quantify the flexoelectric behavior. It will be important to measure single crystals in the ceramic systems which have been studied and to characterize the converse effect as a check of the measured values.
© *2006 Springer Science + Business Media, Inc.*

## 1. Introduction

Flexoelectricity describes the generation of electric polarization in an insulating solid by the application of an elastic strain gradient. The phenomenon is characterized by the tensor relationship

$$P_1 = \mu_{ijkl} \frac{\partial S_{ij}}{\partial x_k} \tag{1}$$

Where

$P_1$ is the component of resultant polarization

$\mu_{ijkl}$ the flexoelectric coefficients, a fourth rank polar tensor

$S_{ij}$ the component of the elastic strain

$x_k$ the direction of the gradient in $S$.

The $\mu_{ijkl}$ have the same symmetry as the electrostriction constants $Q_{ijkl}$ so that for a cubic crystal the non-zero components are $\mu_{1111}$, $\mu_{1122}$, $\mu_{1212}$ or in matrix notation $\mu_{11}$ $\mu_{12}$ and $\mu_{44}$.

The first discussion of electric polarization induced in a centric crystal by inhomogeneous deformation is by Kogan [1]. The phenomenon was named flexoelectricity by Indenbom [2] by analogy with charge separation in non piezoelectric liquid crystals. The effect in soft elastomers was explored by Marvan [3] who still is active in the field. The first comprehensive theoretical discussions are by Tagantsev [4, 5], which underscore the complexity and give the first clear indication of the distinction between static and dynamic coefficients.

It is perhaps not surprising that practical measurement of flexoelectric coefficients languished as it was universally recognized that for simple homogeneous insulating solids the effect was very small with $\mu_{ij} \sim 10^{-10}$ to $10^{-11}$ C/m. Theory [6] predicted four contributors to the effect:

(1) A bulk static flexoelectric effect $\sim 10^{-10}$ C/m

(2) A bulk dynamic coefficient made up from two parts each $\sim 10^{-10}$ C/m

(3) A surface flexoelectric coefficient also of order $\sim 10^{-10}$ C/m

0022-2461 © *2006 Springer Science + Business Media, Inc.*
DOI: 10.1007/s10853-005-5916-6

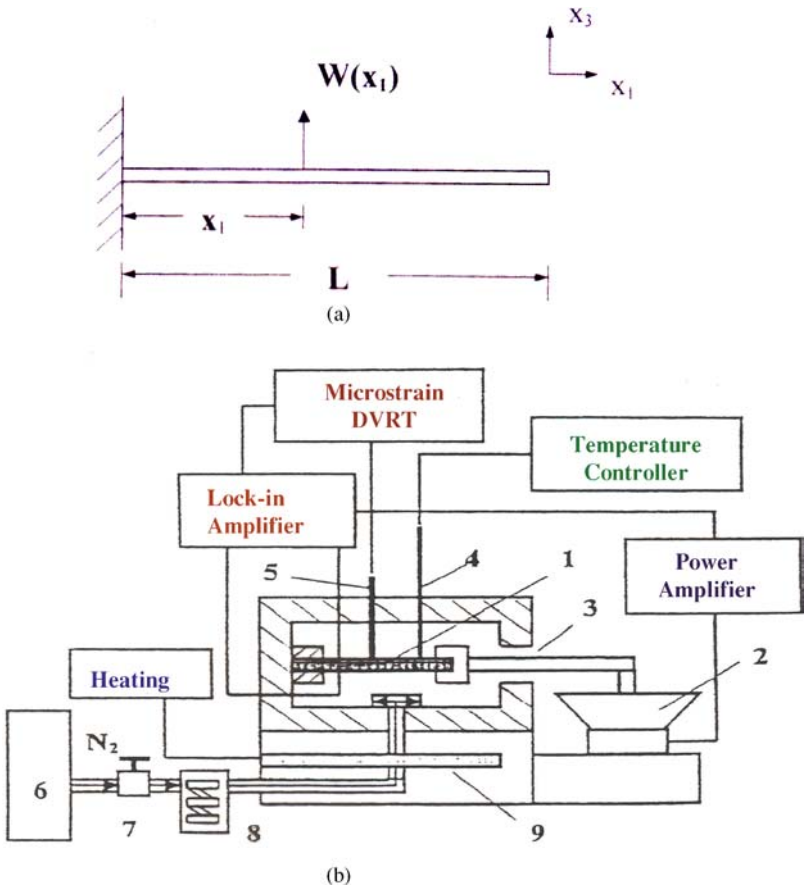


*Figure 1* (a) Typical ceramic bar sample: ceramic bar 76.3×12.7×2.5 mm indicating measuring coordinate directions. (b) Experimental setup for the dynamic measurement of temperature dependence of flexoelectric $\mu_{12}$. 1. PMN bar; 2. Loudspeaker; 3. Driving arm; 4. Thermocouple; 5. Microstrain transducer core; 6. High purity nitrogen; 7. Gas Flow meter; 8. Copper coils immersed in liquid nitrogen; 9. Heating elements.

(4) Surface piezoelectric effect whose magnitude depends markedly on the nature of the surface.

The situation is however more interesting for the paraelectric phase of the soft mode ferroelectric dielectric. Both static and dynamic bulk coefficients become larger in proportion to the enhanced dielectric susceptibility, the surface flexoelectric coefficient does not scale and so becomes unimportant, and the surface piezoelectric effect again depends on surface characteristics. It appeared natural that the place to start would be a high permittivity perovskite and since the laboratory had excellent experience with the relaxor lead magnesium niobate, this was an obvious choice upon which to start.

## 2. Experimental studies

### 2.1. Measuring techniques

Initial focus was on measuring the transverse flexoelectric coefficient $\mu_{12}$ in a range of cubic perovskite high-permittivity ceramics. Both quasi-static and low frequency dynamic techniques have been employed. For dynamic measurement a bar of ceramic of rectangular cross section, clamped at one end was driven in flexure at 1Hz by a small electro-magnetic actuator (Fig. 1). The sample with dimensions in the range 70×12×2 mm is equipped with a set of small circular electrodes equally spaced along the major surface. At each electrode the vertical AC displacement is monitored by a DVRT microstrain transducer and the local charge monitored by a charge amplifier phase locked to the strain generator. Taking the $x_1$ axis along the beam and the $x_3$ axis normal to the electroded surfaces (Fig. 1a), Equation 1 becomes

$$P_3 = \mu_{12}\frac{\partial S_{11}}{\partial x_3} \tag{2}$$

$P_3$ is derived from the charge and electrode area $\frac{\partial S_{11}}{\partial x_3}$ from the local curvature.

The advantage of the flexure method is that there is a neutral axis down the middle of the beam so that any residual piezoelectricity cancels out. Asymmetry can be checked by inverting the beam which makes no difference to the flexoelectric signal but would be changed by piezoelectric asymmetry.

For static measurement the classic four point bending configuration was used (Fig. 2) and the resulting charge measured by electrometer. Here the objective was to

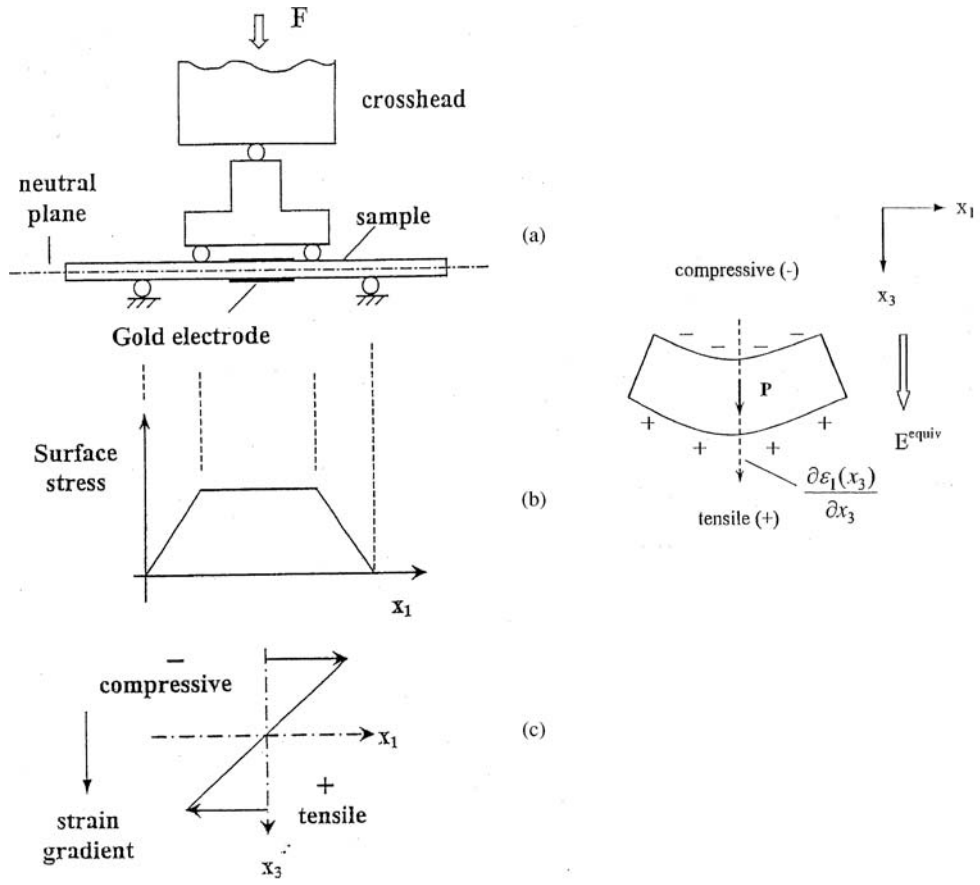


*Figure 2* (a) Experimental arrangement for the static measurement of flexoelectric $\mu_{12}$ to high elastic stress levels. (b) Transverse stress profile for the four point bending experiment. (c) Illustration of the transverse strain gradient. Compressive in upper and tensile in the lower surface. (d) Sketch indicating the expected charge separation due to flexoelectric $\mu_{12.}$.

measure the effective $\mu_{12}$ for the centric $\infty\ \infty$ m symmetry of the unpoled ferroelectric ceramic and examine the possibility of a ferroelastic domain contribution to this response at high stress levels where obvious ferroelastic shape change could be observed.

To measure the longitudinal coefficient $\mu_{1111}$, which is the most important for composite development, an AC Instron type 5866 was adapted to generate cyclic longitudinal stress at 0.5 Hz. The set up is shown schematically in plan and elevation in Fig. 3 and photographs of the holder, environment chamber and sample in Fig. 4. The sample was configured as a truncated triangle of constant width, to generate a uniform vertical stress gradient (Fig. 4c), and for ease of alignment the triangulated stressing jig (Fig. 3b) was developed. The charge release was measured by a charge amplifier phase locked to the AC drive of the Instron system.

## 2.2. Choice of materials

In order to permit a wide range of dielectric permittivities to be studied it was desirable to pick systems with a high weak-field dielectric permittivity maximum at a temperature $T_m$ close to room temperature. For this reason the compound Lead magnesium niobate $Pb(Mg_{1/3}Nb_{2/3})O_3$ (PMN) and the solid solution $Ba_{0.67}Sr_{0.33}TiO_3$ (BST) were chosen for initial study. Above the dielectric maximum both are in cubic point group $m\bar{3}m$ with $\mu_{11}$ $\mu_{12}$ and $\mu_{44}$ the only non-zero flexoelectric coefficients. PMN is the classic prototypic perovskite ferroelectric relaxor. BST is a near approximation to the soft-mode paraelectric, modified by order: disorder near $T_c$ but largely free from lower frequency dielectric dispersion.

For the simple unpolarized ferroelectric perovskite ceramic in texture symmetry $\infty\ \infty$ m, the choice is obviously very much broader. Because of the surprisingly large difference found between PMN and BST, it was decided to choose one lead containing and one non-lead ceramic. An excellent source for the soft lead zirconate titanate PZT 5H close at hand was TRS ceramics State College. For the lead-free ceramic barium titanate ($BaTiO_3$) is an obvious choice. Now however, since the ferroelectric 90° wall behavior was of interest a coarse grained (5–10 $\mu$m) microstructure was required and samples to this specification were fabricated in the laboratory. With the need for long bar-shaped samples and a severely

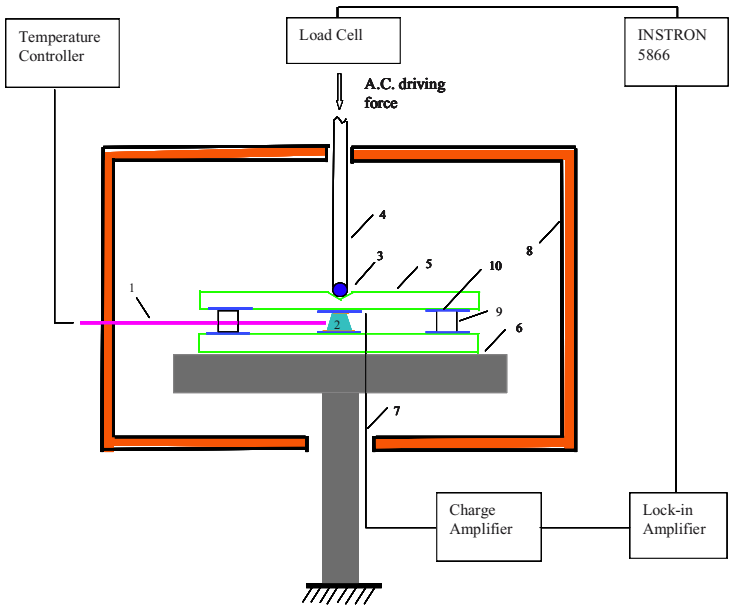


(a)

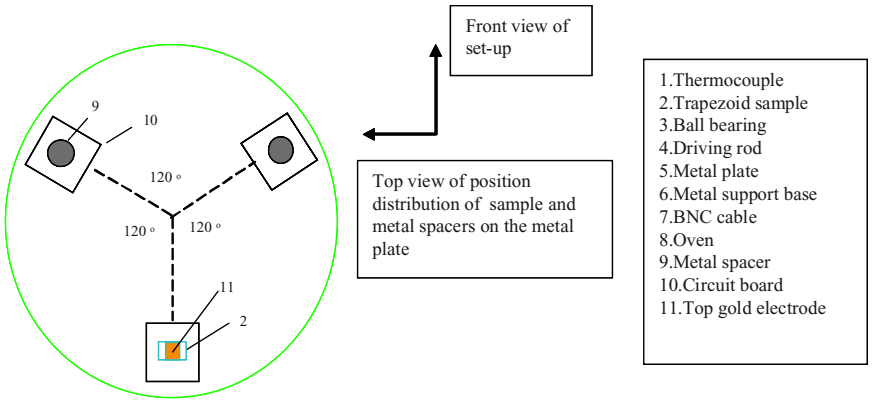


(b)

*Figure 3* Schematic diagram of the arrangement used for measurement of flexoelectric $\mu_{11}$ as a function of temperature.

constrained budget, ceramic samples had to suffice, however at least for PMN and $BaTiO_3$ single crystals should be measured.

## 2.3. Measurements of flexoelectric $\mu_{12}$

Detailed measurements for PMN, BST and PZT 5H have already been published [7–11], so only a brief synopsis of the key features will be reported.

In both PMN (Fig. 5) and in BST (Fig. 6) the enhancement of $\mu_{12}$ with increasing $\epsilon_\omega$ is clearly evident. Over the intermediate range for $\epsilon_\omega$ between 3000 to 11000 both materials follow the prediction by Tagantsev [5] that

$$\mu_{12} = \gamma \chi_{33} \left(\frac{e}{a}\right) \tag{3}$$

where $\chi_{33}$ is the weak field susceptibility. In both these high-permittivity dielectrics $\chi_{33} = \epsilon_\omega$

$e$ is the electron charge

$a$ the unit cell dimension

$\gamma$ a constant.

For PMN $\gamma$=0.65 close to the unity value predicted, but in BST $\gamma$=9.3 much larger than expected.

The fit to Equation 3 in both materials is evidenced in Fig. 7. The enhancement above $\epsilon_\omega \sim 11000$ in BST correlated closely with a departure in $\frac{1}{\varepsilon_\omega}$ from Curie–Weiss behavior and one suspects the introduction of a new polarizability associated with the occurrence of a few ferroelectric macro-domains. The reason for the drop in $\mu_{12}$ at permittivity values below 3000 is unclear as the sensitivity is quite adequate for much lower level signals.

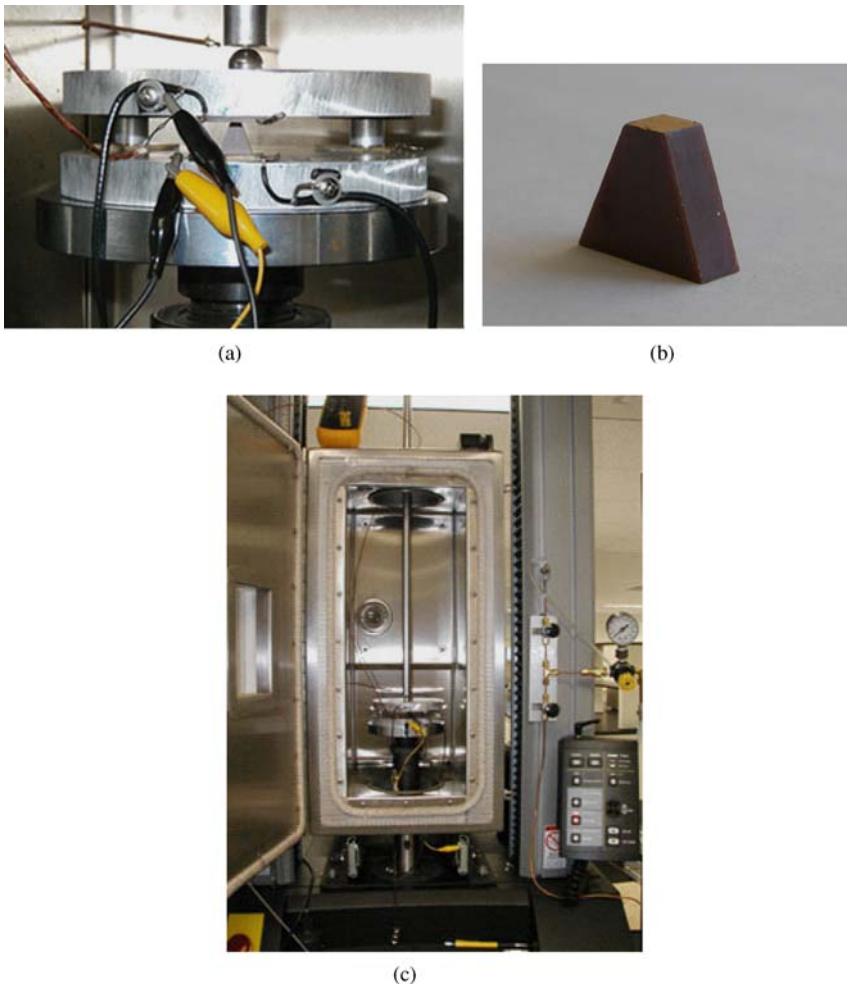


*Figure 4* Photographs of the arrangement used for $\mu_{11}$ measurements. (a) Sample holder and stressing jig. (b) Typical electroded sample. (c) Environment chambers for holding the sample.

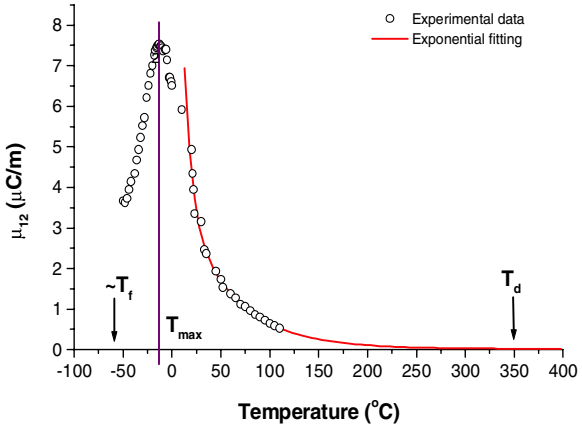


*Figure 5* Flexoelectric $\mu_{12}$ in $Pb(Mg_{1/3}Nb_{2/3})O_3$ Ceramic as a function of temperature in the macro-cubic domain above the dielectric $T_{max}$ measured at 1 Hz.

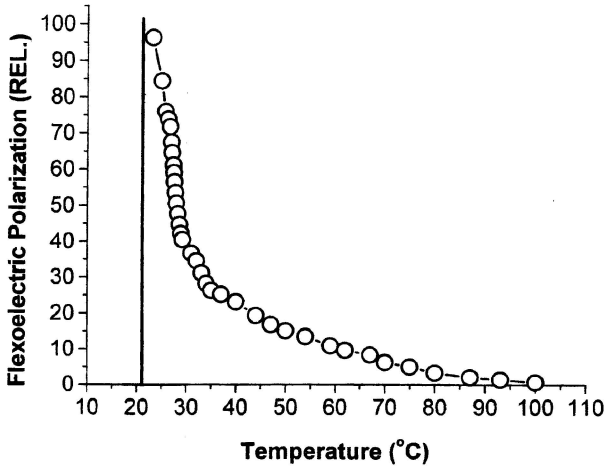


*Figure 6* Flexoelectric polarization as a function of temperature in $(Ba_{0.67}Sr_{0.33})\ TiO_3$ ceramic, measured at 1 Hz. The vertical solid line indicates the Curie Temperature in this composition.

Initial objectives for the quasi-static flexure studies were to see whether the pattern of ferroelectric domains in an unpoled ferroelectric ceramic below $T_c$ would markedly influence $\mu_{12}$. At stress levels capable of driving ferroelastic domain walls, whether there would be an extrinsic domain contribution to response, and if so, whether the strain

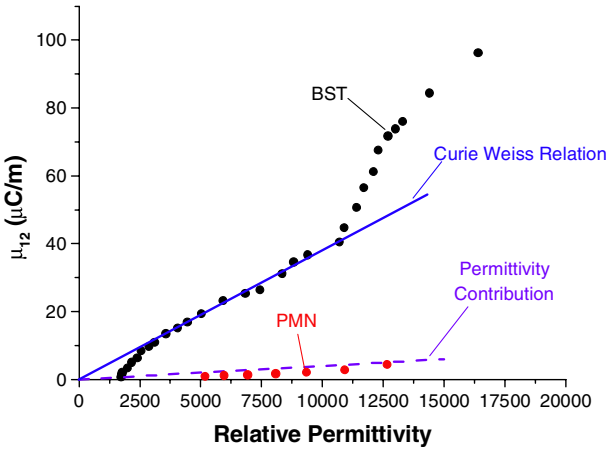


*Figure 7* Comparison of Flexoelectric $\mu_{12}$ as a function of the dielectric permittivity$\epsilon_3$ in $Pb(Mg_{1/3}Nb_{2/3})O_3$ and $Ba_{0.67}Sr_{0.33}TiO_3$.

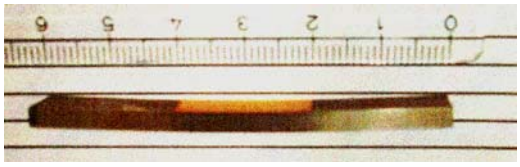

*Figure 8* Illustration of the residual ferroelectric curvature in a typical PZT-5H bar after high stress four-point bend test. Clear indication that the sample has experienced ferroelastic domain wall motion.

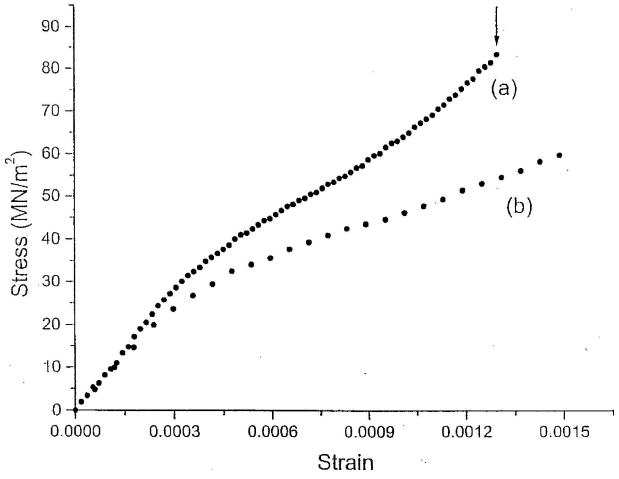


*Figure 9* Surface strain as a function of surface stress during 4-point bending test. (a) Cross head speed 1 mm/min. (b) Crosshead speed 0.2 mm/min. Note the onset of time dependent softening due to ferroelastic:ferroelectric domain wall motion.

gradient could pole the ceramic to a piezoelectric state.

Residual curvature after high 4 point loading (Fig. 8) gives clear evidence of ferroelastic domain rearrangement, and the change in elastic stiffness at surface strain around $s_{11} \sim 0.0003$ (Fig. 9) suggests the onset of ferroelastic domain wall motion. This surface strain level corresponds to a strain gradient of 0.2 $m^{-1}$ and it is exciting to see in Fig. 10 the clear change of slope in the induced polarization corresponding to a change of $\mu_{12}$ from 0.5 to 2 $\mu$C/m clear evidence of an extrinsic domain contribution to the flexoelectric response. Careful testing by both phase sensitive $d_{33}$ meter and IEEE resonance method however failed to show any evidence of an induced piezoelectric poling even after subjecting the samples to a maximum gradient of 1 $m^{-1}$.

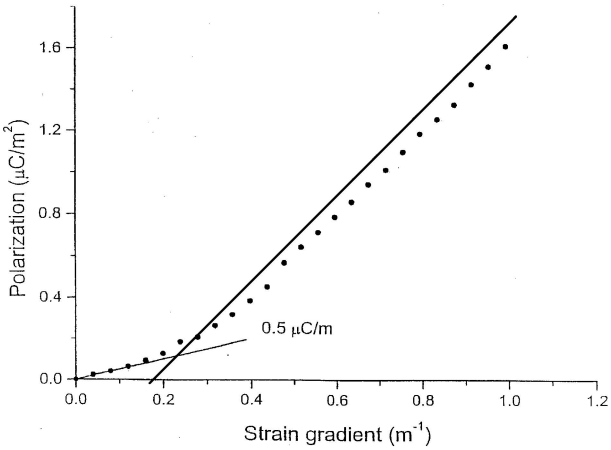


*Figure 10* Flexoelectric polarization $P_3$ driven by the gradient in elastic strain $S_1$ Note the onset of enhanced $\mu_{12}$ above the strain level needed to drive ferroelectric domain wall motion.

In the high-temperature paraelectric phase where the response is just intrinsic it is interesting to see that for $BaTiO_3$ $\gamma = 11.4$.

## 2.4. Summary of results for $\mu_{12}$

Lead magnesium niobate $PbMg_{1/3}Nb_{2/3}O_3$ $\gamma = 0.65$
Lead zirconate titanate PZT 5H Intrinsic $\gamma = 0.57$
Barium Strontium titanate $Ba_{0.67}Sr_{0.33}TiO3$ $\gamma = 9.3$
Pure barium titanate ceramic $BaTiO_3$ $\gamma = 11.4$
For PZT 5H in the ferroelectric phase
Intrinsic $\mu_{12} = 0.5$ $\mu$C/m Extrinsic 1.5 $\mu$C/m
For $BaTiO_3$ in the ferroelectric tetragonal phase Intrinsic $\mu_{12} = 5.5$ $\mu$C/m Extrinsic 30.2 $\mu$C/m

## 2.5. Measurements of flexoelectric $\mu_{11}$

Initial studies have been focused on BST at the $(Ba_{0.67}Sr_{0.33})TiO_3$ composition and on lead strontium titanate (PST) at the $(Pb_{0.3}\ Sr_{0.7})TiO_3$ composition. As with BST, the PST composition is chosen to have $T_m$ just below room temperature. It has classical Curie-Weiss behavior from high temperature to within 15°C of $T_m$ with no low radio frequency dispersion and no evidence of relaxor ferroelectric character.

For the BST, again as expected, there is a good proportionality between the gradient and the induced polarization (Fig. 11) which leads to a well defined $\mu_{11}$ that

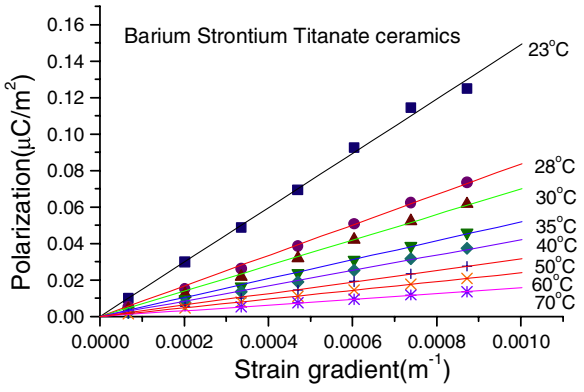


Fig. 11

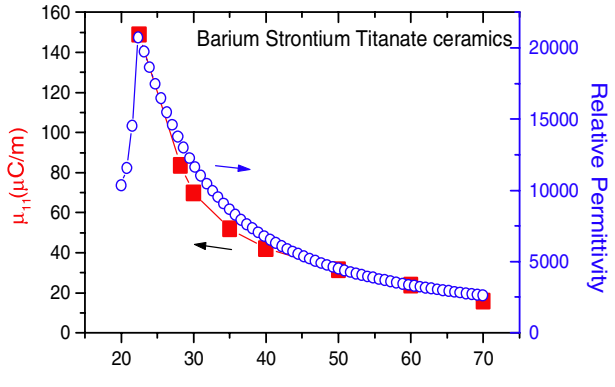


Fig. 12

*Figures 11 and 12* AC Instron measurement of $\mu_{11}$ as a function of temperature $(Ba_{0.67}Sr_{0.33})TiO_3$ Ceramic. Frequency 0.5 Hz Gradient range 0 to 0.00088 $m^{-1}$.

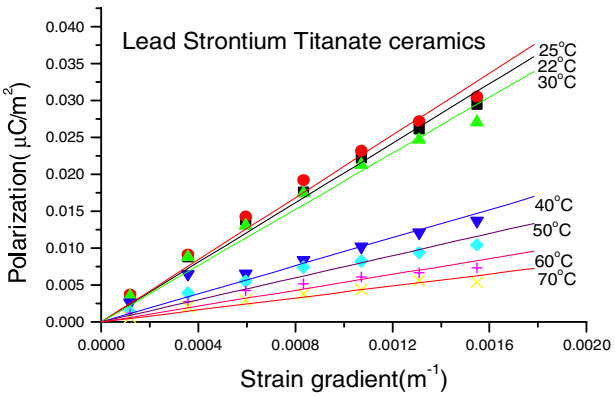


Fig. 13

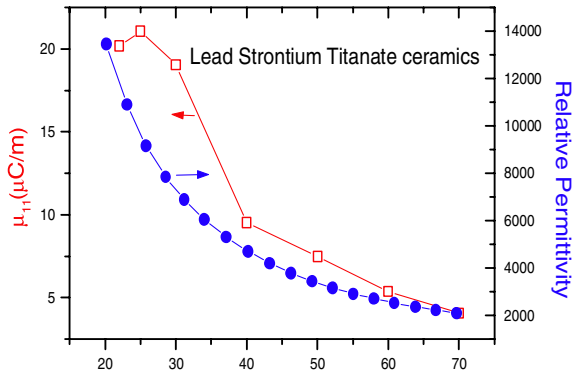


Fig. 14

*Figures 13 and 14* AC Instron Measurement of $\mu_{11}$ as a function of temperature in $(Pb_{0.03}Sr_{0.07})$ $TiO_3$ ceramic frequency 0.5 Hz Gradient range 0 to $0.0015_5$ $m^{-1}$.

also follows the proportionality to dielectric permittivity suggested in Equation 3 (Fig. 12) with a $\gamma$ value of 18.3.

In PST, the general trend is the same, with good proportionality to the gradient level, (Fig. 13), but the tracking with dielectric permittivity is not so precise (Fig. 14). The mean $\gamma$ value is 4.5.

Again it appears that the lead based compound has a significantly lower $\gamma$ than the BST for $\mu_{11}$ even though it is not relaxor, but in both BST and PST it may be noted that the linear relation to Є breaks down as $T$ approaches $T_c$ with $\mu_{11}$ climbing more rapidly with decreasing temperature suggesting the intervention of a new polarization mechanism. Currently, although different samples of the same composition give similar values at the same temperature we must regard both the measured $\mu_{11}$ and $\gamma$ values as preliminary as there is a spurious charge generation in the system which must be tracked down and corrected.

## 3. Thermodynamics of flexoelectricity

The constitutive equations for flexoelectricity take the form

$$P_i = \eta_{ij} E_j + \mu_{ijkl} \frac{\partial S_{kl}}{\partial x_j} \tag{4}$$

And

$$T_{k1} = c_{ijkl} S_{ij} - \mu_{ijkl} \frac{\partial E_i}{\partial x_j} \tag{5}$$

Where

$P_i$ are the polarization components
$E_i$,$E_j$ the electric field component
$T_{k1}$ the elastic stress components
$S_{ij}$ the elastic strain components
$\eta_{ij}$ the dielectric susceptibility
$c_{ijkl}$ the elastic constant
$\mu_{ijkl}$ the flexoelectric constants
$\partial S_{kl}/\partial \chi$ is the strain gradient in the $j^{th}$ direction
$\partial E_i/\partial \chi_j$ is the electric field gradient in the $j$th direction

For the electric polarization generated by an elastic strain gradient Equation 4 clearly reduces to

$$E_j = 0 \quad P_i = \mu_{ijkl} \frac{\partial S_{kl}}{\partial x_j}$$

which is the equation we have used for the direct flexoelectric effect.

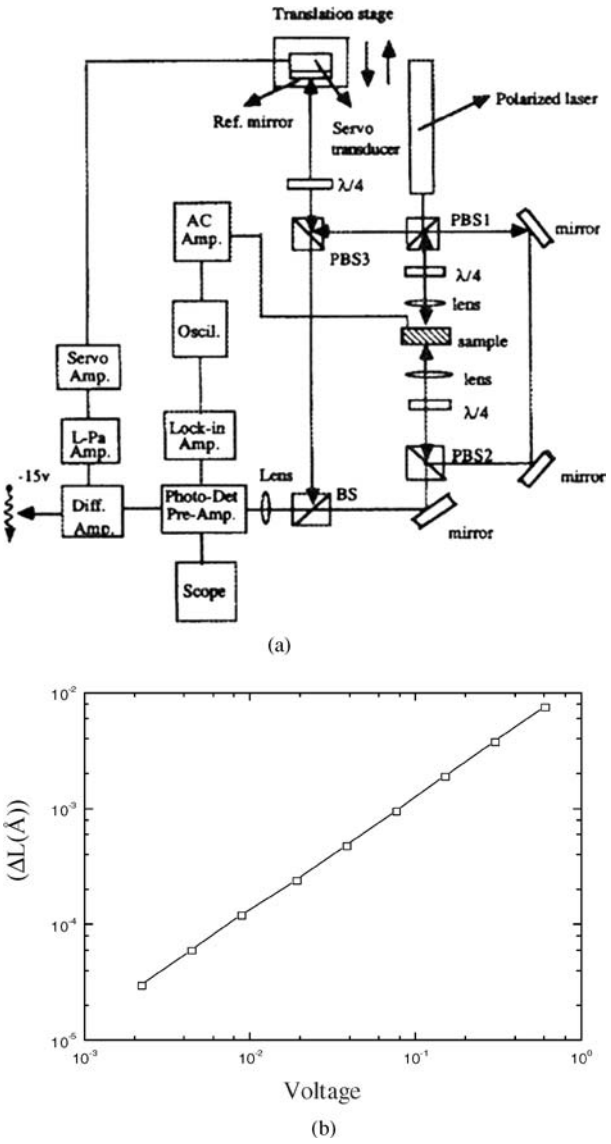


*Figure 15* (a) Schematic of the Ultra-Sensitive laser double beam interferometer to be used for converse flexoelectric displacement measurements. (b) Calibration curve for the dilatometer using piezoelectric lithium niobate.

For the case (5) under zero applied stress Equation 5 reduces to

$$T_{\rm kl} = 0 \quad c_{ijkl} S_{ij} = \mu_{ijkl} \frac{\partial E_i}{\partial x_j}$$

which clearly represents the converse effect i.e. the change of elastic strain at zero elastic stress generated by an electric field gradient.

### 3.1. Converse flexoelectric effect

So far we know of no attempts to measure the converse flexoelectric effect. However, interferometric techniques for measuring exceedingly small strains are very well developed and capable of measuring field induced displacements of order $10^{-4}$ Å[12]. The example we have is the system illustrated schematically in Fig. 15a. In this system, the photo-detector is phase locked to the low sample driving frequency. Drifts due to thermal changes and low frequency vibrations are taken out by the compensation mirror driven by a piezoelectric actuator. Stability and sensitivity of the system can be judged by the Calibration Curve in Fig. 15b which is linear down to $2\times10^{-5}$ Å.

Unfortunately, initial studies were frustrated when it proved impossible to read the flexoelectric signal at frequency $\omega$ against the much larger signal at $2\omega$ generated by electrostriction, one of the higher order effects not considered in Equation 5. To overcome this difficulty the sample is being miniaturized to steepen the gradient in $E$ and the compensator illustrated in Fig. 16 is under construction.

TABLE I None zero components of piezoelectric $d$ constant $d_{ij}$ in matrix notation. In all groups the $\infty$ axis is taken as $x_3$; the axes $x_1$, $x_2$ are perpendicular to $x_3$ and to each other, but otherwise in arbitrary orientation

**Matrices of $d_{ijk}$ in Curie groups which are piezoelectric**

$\infty$

| | | | | | |
|---|---|---|---|---|---|
| 0 | 0 | 0 | $d_{14}$ | $d_{15}$ | 0 |
| 0 | 0 | 0 | $d_{14}$ | $-d_{14}$ | 0 |
| $d_{31}$ | $d_{31}$ | $d_{33}$ | 0 | 0 | 0 |

$\infty 2$

| | | | | | |
|---|---|---|---|---|---|
| 0 | 0 | 0 | $d_{14}$ | 0 | 0 |
| 0 | 0 | 0 | 0 | $-d_{14}$ | 0 |
| 0 | 0 | 0 | 0 | 0 | 0 |

$\infty m$

| | | | | | |
|---|---|---|---|---|---|
| 0 | 0 | 0 | 0 | $d_{15}$ | 0 |
| 0 | 0 | 0 | $d_{15}$ | 0 | 0 |
| $d_{31}$ | $d_{31}$ | $d_{33}$ | 0 | 0 | 0 |

## 4. Application to a piezoelectric composite

### 4.1. Introduction

The Penn State studies of flexoelectricity were initiated by discussions[1] on textures symmetries which pointed up the characteristic forms representing the Curie groups that are piezoelectric (Fig. 17a). If such forms are arranged in an orderly manner, as in Fig. 17b, to form a two phase composite, and both phases are insulators, even if neither phase is piezoelectric the composite ensemble must exhibit piezoelectricity. Further, if in all groups the $\infty$ axis is taken as $x_3$ the matrices of the non-zero piezoelectric constants will be as in Table I.

For the $\infty$m symmetry, discussing the possible charge separation mechanisms to account for the symmetry

[1]The Penn State flexoelectric program was initiated through discussion with Professor J. Fousek on possible mechanisms which could impart charge separation under elastic stress in textures symmetry $\infty$ m.

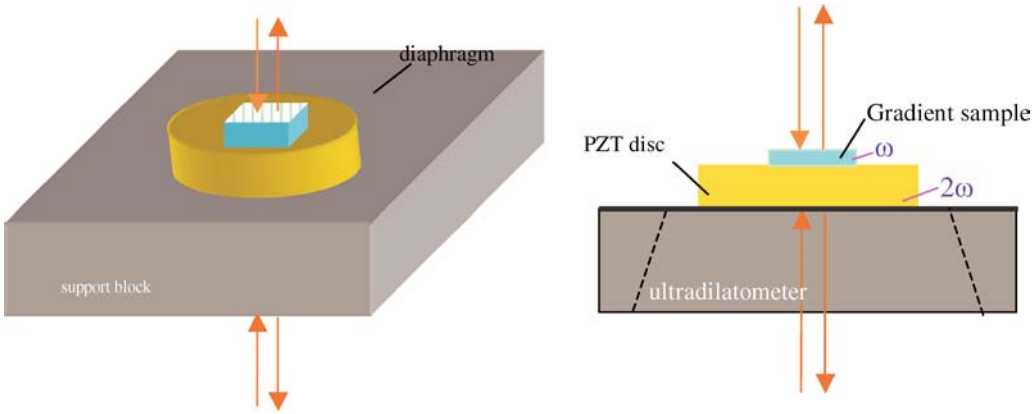


*Figure 16* Proposed sample arrangement for the converse measurement of $\mu_{11}$. Sample driven at frequency $\omega'$, shaped to generate a strong field gradient in Ez Gradient generates a deformation at frequency $\omega'$, but electrostriction generates a much stronger deformation at $2\omega'$ PZT disc is driven at $2\omega'$ in anti-phase to the electrostriction deformation. Drive is varied to cancel out the total AC deformation at $2\omega'$ High sensitivity of the ultra-dilatometer can now be used to measure the deformation at frequency without perturbation by the much larger electrostriction signal.

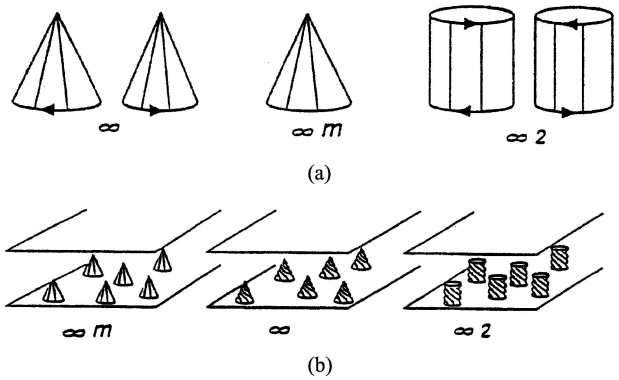


*Figure 17* (a) Characteristic forms representing symmetry of the Curie groups which allow for piezoelectricity. (b) Simple models of 0–3 composites allowing for piezoelectricity. There is an infinite number of shapes of the 0-constituent that could be tested for a maximum response.

required behavior, it was evident that even if nonpiezoelectric the two phases differ in elastic properties so that the conical shape automatically gives rise to an axial stress gradient, even if the composite is subjected to a uniform stress. The gradient will then act through the flexoelectric effect to produce charge separation.

Remembering that symmetry only dictates what must be present (or absent), and nothing as to the magnitude, the natural question was whether flexoelectricity could lead to usable piezoelectric properties in a properly configured composite. Hence, the need to measure the $\mu_{ijkl}$ in materials likely to have large values of these constants.

To illustrate the potential, take for example the square truncated pyramid as in Fig. 18a as the element in a composite sheet (Fig. 18b). Suppose the upper square face has a side of length $a_1$, and the lower a length $a_2$ and the side wall is configured so that $a_2$ is a linearly increasing function of d the depth from $a_1$ to $a_2$. For a force F applied normal to upper and lower surfaces. Stress in the upper surface will be $T_{3(1)} = F/a_1^2$ and will give rise to a strain $S_{3(1)}$ given by$S_{3(1)} = F/a_1^2 c_{11}$ where $c_{11}$ is the elastic constant of the truncated pyramid.

Similarly for the lower surface $T_{3(2)} = F/a_2^2$ and $S_{3(2)} = F/a_2^3 c_{11}$

Since the side walls are configured to make $a^2$ a linear function of $d$

$$\frac{\partial S_3}{\partial d} = \frac{S_{3(1)} - S_{3(2)}}{d} = \frac{F\left(\frac{1}{a_1^2} - \frac{1}{a_2^2}\right)}{dc_{11}}$$

If the pyramid material has a flexoelectric coefficient $\mu_{11}$ then

$$P_3 = \mu_{11}\frac{\partial S_3}{\partial d_3} = \mu_{11}\frac{F\left(\frac{1}{a_1^2} - \frac{1}{a_2^2}\right)}{dc_{11}} = \mu_{11}\frac{\frac{a_2^2 - a_1^2}{a_1^2}}{dc_{11}} \bullet \frac{F}{a_2^2}$$

i.e.

$$P_3 = \mu_{11}\frac{\left(\frac{a_2^2 - a_1^2}{a_1^2}\right)}{dc_{11}}T3$$

but for a piezoelectric sheet

$$P_3 = d_{33}T_3$$

So that

$$d_{33} = \mu_{11}\frac{\left(\frac{a_2^2 - a_1^2}{a_1^2}\right)}{dc_{11}}$$

For BST at room temperature $\mu_{11} \sim 100\ \mu$C/m

$$c_{11} = 1.66 \times 10^{11}\ \mathrm{N}/m^2$$

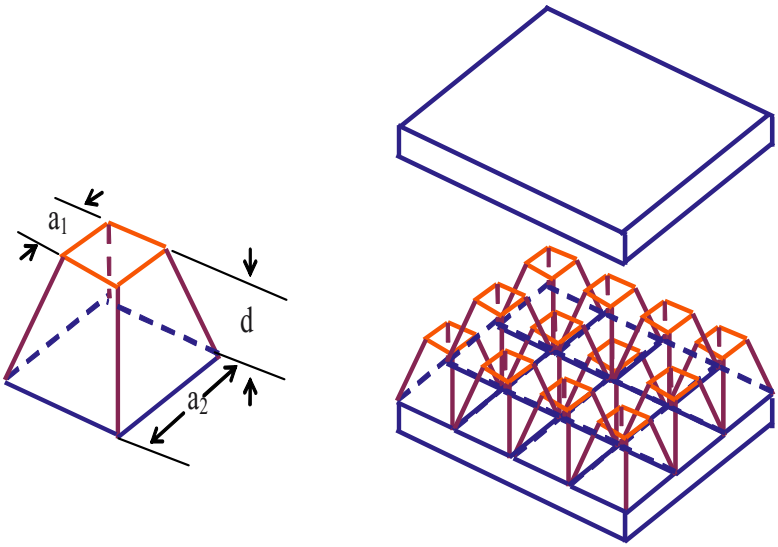


(a) (b)

*Figure 18* Proposed composite to generate piezoelectric response from flexoelectric polarization. (a) Individual truncated pyramidal building block from BST strongly flexoelectric stiff ceramic. (b) Composite arrangement of individual elements. Second phase in initial study will be air. Later a soft polymer. Since the vertical gradient of strain is uniform down the pyramids the whole upper surface may be electrode for charge collection.

for $a_1 = 50\ \mu$m $a_2 = 250\ \mu$m $d = 250\ \mu$m $d_{33} \approx 60$ pC/N
Scaling down $a_1 = 5\ \mu$ m, $a_2 = 25\ \mu$m $d = 25\ \mu$m $d_{33} \approx 600$ pC/N.
A quite useful level at not impossibly small dimensions for the composite.

## 5. Future prospects

Immediate objectives of the current program are to uncover the spurious charge generation mechanisms in the $\mu_{1111}$ studies on BST and PST and to fabricate a coarse scale composite of the form described in 4 above to just demonstrate proof of principle. We believe that the problem of generating a completely uniform axial stress on a very stiff ceramic may be the source of the spurious charge generation that has plagued our $\mu_{11}$ measurements.

It is associated with the difficulty of generating an elastic equipotential surface, which was a major headache in earlier studies of the converse electrostrictive constants in simple solids obtained by measuring the uniaxial stress dependence of the dielectric susceptibility. Steps to be taken to explore the problem include elastic matching of piston and sample to avoid Poisson Ratio effects, soft elastic gaskets sealed at high stress levels, and if necessary, integrated with fired-in elastically matching electrodes.

For proof of principle a sub millimeter composite has already been fabricated and the assembly is in final stages. We hope that it will be possible to make the first measurements of the converse effect as the system is already fabricated, but pressure on the use of the ultra dilatometer is heavy and the current program may run out before measurements can be completed. We believe the topic bristles with intriguing possible longer-range opportunities.

Clearly, grain boundaries are a worrisome source of unneeded complexity, and the random crystallite arrangement can give rise to elastic inhomogeneity even in cubic systems. On the compounds already studied measurements should be carried out on single crystals to ascertain the validity of these concerns.

As was the case with electrostriction in simple low-permittivity solids, essential validation of the measured values is in close agreement between direct and converse measurements. Flexoelectric deformation associated with the strain generated by electric field gradient must be measured to confirm direct measurement.

If the piezoelectric composite demonstration validates the principle, it is possible to conceive of composites on a much finer scale which would have exciting properties. Further, it is not unreasonable to believe that systems could be developed where a strong strain gradient would develop under uniform stress but be unaccompanied by a strong polarization gradient under uniform electric field yielding composites with direct but no converse piezoelectricity and vice versa.

We believe that much remains to be done practically; also with current rapid progress in ab-initio theory for the perovskite it is clear that more refined theoretical approaches are certainly becoming accessible.

## References

1. S. M. KOGAN, *Sov. Phys. Solid State* **5** (1964) 2069.

2. V. L. INDENBOM, E. B. LOGINOV and M. A. OSIPOV, *Kristalografija* **26** (1981) 1157.
3. M. MARVAN and A. HAVRANEK, *Science* **78** (1988) 33.
4. A. K. TAGANTSEV, *Phys. Rev. B* **34** (1986) 5883.
5. *Idem.*, *Phase Trans.* **35** (1991) 119.
6. *Idem.*, *Sov. Phys. JETP* **61**(6) (1985) 1246.
7. W. MA and L. E. CROSS, *Appl. Phys. Lett.* **78** (2001) 2920.
8. *Idem.*, *ibid.* **79** (2001) 4420.
9. *Idem.*, *ibid.* **81** (2002) 3440.
10. *Idem.*, *ibid.* **82** (2003) 3293.
11. *Idem.*, *ibid.*. **86** (2005) 072905.
12. W. Y. PAN and L. E. CROSS, *Rev. Sci. Inst.* **60**(8) (1989) 2701.